J|A|C|S ARTICLES

Published on Web 05/15/2009

Rapid in Situ Generation of Two Patterned Chemoselective Surface Chemistries from a Single Hydroxy-Terminated Surface Using Controlled Microfluidic Oxidation

Abigail Pulsipher, Nathan P. Westcott, Wei Luo, and Muhammad N. Yousaf*

Department of Chemistry and Carolina Center for Genome Science, University of North Carolina at Chapel Hill, Chapel Hill, North Carolina 27599-3290

Received December 1, 2008; E-mail: mnyousaf@email.unc.edu

Abstract: In this work, we develop a new, rapid and inexpensive method to generate spatially controlled aldehyde and carboxylic acid surface groups by microfluidic oxidation of 11-hydroxyundecylphosphonic acid self-assembled monolayers (SAMs) on indium tin oxide (ITO) surfaces. SAMs are activated and patterned using a reversibly sealable, elastomeric polydimethylsiloxane cassette, fabricated with preformed micropatterns by soft lithography. By flowing the mild oxidant pyridinium chlorochromate through the microchannels, only selected areas of the SAM are chemically altered. This microfluidic oxidation strategy allows for ligand immobilization by two chemistries originating from a single SAM composition. ITO is robust, conductive, and transparent, making it an ideal platform for studying interfacial interactions. We display spatial control over the immobilization of a variety of ligands on ITO and characterize the resulting oxime and amide linkages by electrochemistry, X-ray photoelectron spectroscopy, contact angle, fluorescence microscopy, and atomic force microscopy. This general method may be used with many other materials to rapidly generate patterned and tailored surfaces for studies ranging from molecular electronics to biospecific cell-based assays and biomolecular microarrays.

Introduction

The ability to tailor materials with self-assembled monolayers (SAMs) to generate diverse chemical and physical properties has proven to be important for a range of research fields, such as biomedical engineering, organic catalysis, molecular electronics, and cell biology.[1] SAMs of alkanethiolates on gold represent one of the most well-studied surface chemistry systems. The major advantages of SAMs on gold include the inherent conductivity of gold that allows substrate compatibility with a variety of surface characterization techniques. Alkanethiols are also synthetically flexible or commercially available, providing opportunities to tailor materials for a range of applications.[2] In addition to the direct synthesis of alkanethiols, a number of convergent interfacial chemoselective strategies including Diels−Alder conjugation,[3] Click chemistry,[4] quinone and aldehyde coupling,[5] Staudinger ligation,[6] and Michael addition[7] have been developed to immobilize and present a variety of ligands on the surface. There have also been numerous lithographic approaches used to pattern SAMs of alkanethiols on gold, such as photolithography,[8] electron-beam,[9] X-ray,[10] extreme UV,[11] and dip pen[12] nanolithography. Disadvantages of these strategies include the lack of commercially available molecules containing the desired alkanethiol tail group, the

(1) (a) Zhi, Z.-L.; Laurent, N.; Turnbull, J. E. *ChemBioChem* **2008**, *9*, 1568–1575. (b) Park, T. H.; Shuler, M. L. *Biotechnol. Prog.* **2003**, *19*, 243–253. (c) Panda, S.; Sata, T. K.; Hampton, G. M.; Hogenesch, J. B. *Trends Cell Biol.* **2003**, *13*, 151–156. (d) Hoover, D. K.; Lee, E.-J.; Chan, E. W. L.; Yousaf, M. N. *ChemBioChem* **2007**, *16*, 1920–1923. (e) Barrett, D. G.; Yousaf, M. N. *Angew. Chem., Int. Ed.* **2007**, *46*, 7437–7439. (f) Laurent, N.; Voglmeir, J.; Wright, A.; Blackburn, J.; Wong, S. C.; Gaskell, S. J.; Flitsch, S. L. *ChemBioChem* **2008**, *6*, 883–887. (g) Chan, E. W. L.; Yousaf, M. N. *ChemPhysChem* **2007**, *8*, 1469–1472.

(2) (a) Hahn, M. S.; Taite, L. J.; Moon, J. J.; Rowland, M. C.; Ruffino, K. A. I.; West, L. J. *Biomaterials* **2006**, *27*, 2519–2905. (b) Carroll, G. T.; Wang, D. N.; Turro, N. J.; Koberstein, J. T. *Langmuir* **2006**, *22*, 2899–2905. (c) Ryan, D.; Parviz, B. A.; Linder, V.; Semetey, V.; Sia, S. K.; Su, J.; Mrksich, M.; Whitesides, G. M. *Langmuir* **2004**, *20*, 9080–9088. (d) Pale-Grosdemange, C.; Simon, E. S.; Prime, K. L.; Whitesides, G. M. *J. Am. Chem. Soc.* **1991**, *113*, 12–20. (e) Dillmore, S. W.; Yousaf, M. N.; Mrksich, M. *Langmuir* **2004**, *20*, 7223–7231.

(3) (a) Yousaf, M. N.; Mrksich, M. *J. Am. Chem. Soc.* **1999**, *121*, 4286–4287. (b) Houseman, B. T.; Huh, J. H.; Kron, S. J.; Mrksich, M. *Nat. Biotechnol.* **2002**, *20*, 270–274. (c) Yousaf, M. N.; Chan, E. W. L.; Mrksich, M. *Angew. Chem., Int. Ed.* **2000**, *112*, 2019–2022.

(4) (a) Kolb, H. C.; Finn, M. G.; Sharpless, K. B. *Angew. Chem., Int. Ed.* **2002**, *40*, 2004–2021. (b) Zhang, Y.; Luo, S.; Tang, Y.; Yu, L.; Hu, K.-Y.; Pei, J.-P.; Zeng, X.; Wang, P. G. *Anal. Chem.* **2006**, *78*, 2001–2008.

(5) (a) Chan, E. W. L.; Park, S.; Yousaf, M. N. *Angew. Chem., Int. Ed.* **2008**, *120*, 6363–6367. (b) Lamb, B. M.; Barrett, D. G.; Westcott, N. P.; Yousaf, M. N. *Langmuir* **2008**, *24*, 8885–8889. (c) Horton, R. C., Jr.; Herne, T. M.; Myles, D. C. *J. Am. Chem. Soc.* **1997**, *119*, 12980–12981.

(6) Watzke, A.; Kohn, M.; Wacker, R.; Schroder, S. L.; Waldmann, H. *Angew. Chem., Int. Ed.* **2006**, *45*, 1408–1412.

(7) Raj, C. R.; Behera, S. *Langmuir* **2007**, *23*, 1600–1607.

(8) Jaeger, C. R. *Lithography: Introduction to Microelectrode Fabrication*; Prentice Hall: Upper Saddle River, NJ, 2002.

(9) (a) Schilp, S.; Ballav, N.; Zharnikov, M. *Angew. Chem., Int. Ed.* **2008**, *47*, 6786–6789. (b) Ballav, N.; Schilp, S.; Zharnikov, M. *Angew. Chem., Int. Ed.* **2008**, *47*, 1421–1424. (c) Schmelmer, U.; Paul, A.; Kuller, A.; Steenackers, M.; Ulman, A.; Grunze, M.; Golzhauser, A.; Jordan, R. *Small* **2007**, *3*, 459–465. (d) Steenackers, M.; Kuller, A.; Ballav, N.; Zharnikov, M.; Grunze, M.; Jordan, R. *Small* **2007**, *10*, 1764–1773.

(10) Klauser, R.; Huang, M. L.; Wang, S. C.; Chen, C. H.; Chuang, T. J.; Terfort, A.; Zharnikov, M. *Langmuir* **2004**, *20*, 2053–2058.

10.1021/ja809380e CCC: $40.75

narrow range of tail groups able to be used with these transformative methods,[13] and the large amounts of irradiation that may ultimately compromise the gold−thiol bond.[14] In situ SAM activation, a simple non-irradiative chemical modification to the tail group of a prepared SAM composed of either commercially available or easily synthesized molecules, represents an alternative strategy for tailoring surfaces.[15] With this approach, the original SAM tail group is rapidly transformed into a complexly patterned and functionalized substrate for subsequent customization with no further synthesis or patterning steps. Also, this method may facilitate access to the functionalizing of other materials that exhibit weaker associations between the headgroup and the surface, as well as SAM molecules incompatible with routine synthesis (e.g., nickel surfaces requiring isocyanide head groups, glass, TiO_2, ITO, and oxidized GaAs surfaces requiring phosphonate, siloxane, or carboxylate head groups).[16]

Although gold-based SAMs are the most flexible model system for studying biointerfacial science, there remain severe long-term stability and biocompatibility issues. The thiol−gold bond is thermally unstable and upon long durations of air exposure may oxidize, damaging the integrity of the monolayer.[17] Gold also efficiently quenches fluorescence and has limited optical transparency properties that reduce its use for fluorescent-based biosensor or cell array technologies.[18] To address these limitations, there has been intense interest in transferring certain surface chemistries developed for gold and glass surfaces to other materials to increase their scope of applications.[19] One such material, indium tin oxide (ITO), is a common material widely used for applications in optoelectronics and is found as the transparent conductive coatings in plasma, touch, and liquid crystal displays, as well as solar cells and organic light emitting diode (OLED) devices.[20] Its high conductivity permits the characterization of ITO with a variety of analytical techniques.[21] Unlike gold, the optical transparency of ITO presents opportunities for studies involving fluorescence and, in particular, research in cell biology that requires live-cell high-resolution fluorescence microscopy to study cell behavior.[22] However, the major limitation of ITO is the inability to tailor the surface with a variety of surface chemistries. Alkyl carboxylates and alkyl phosphonates have been shown to form SAMs on ITO, but the lack of synthetic routes available to append chemical functionalities to these tail groups and to pattern these molecules has limited the overall use of ITO substrates in biosensor and cell biological studies. Currently, methods exist to pattern ITO onto other materials such as glass, aluminum, and silicon for applications in optoelectronics.[23] Microcontact printing has been used to pattern siloxane SAMs on ITO,[24] but direct SAM tailoring through chemical activation of a tail group has remained undeveloped. A methodology that could chemically alter a single phosphonate SAM on ITO to multiple functionalities for subsequent ligand immobilization would be cost-effective and extremely useful. Not only would this strategy circumvent the difficulties encountered in synthesis, but it would also provide a platform to tailor many other materials for a broad range of interests.

Herein, we report a rapid and inexpensive method to activate and generate spatially controlled aldehyde- and carboxylic acid-functionalized SAMs on ITO using microfluidic oxidation from hydroxyl-terminated SAMs on ITO. This system allows for ligand immobilization by two orthogonal strategies originating from an initial hydroxy-terminated alkanephosphonate. Microfluidic patterning provides spatial control of the aldehydes and carboxylic acids formed by oxidation directly on the surface. Through chemoselective conjugation of oxyamine-containing ligands to aldehydes (to generate oximes) and of amine-containing ligands to carboxylic acids (to generate amides), a variety of electroactive and fluorescent molecules were immobilized. The resulting oxime and amide linkages were characterized by electrochemistry, X-ray photoelectron spectroscopy, fluorescence microscopy, contact angle, and atomic force microscopy.

Results and Discussion

The general schematic illustrating the oxidative activation of SAMs on ITO (100 Ω/sq), with controlled generation of aldehyde and carboxylic acid tail groups for subsequent chemoselective ligation, is shown in Figure 1. Following SAM formation of 11-hydroxyundecylphosphonic acid ($H_2O_3PC_{11}OH$, **1**, Scheme 1) on ITO, a polydimethylsiloxane (PDMS) microfluidic cassette (fabricated using standard soft lithographic

(11) (a) Brandow, S. L.; Chen, M.-S.; Aggarwal, R.; Dulcey, S. C.; Calvert, J. M.; Dressick, W. J. *Langmuir* **1999**, *15*, 5429–5433. (b) Carter, D. J. D.; Pepin, A.; Schweizer, M. R.; Smith, H. I. *J. Vac. Sci. Technol. B* **1997**, *15*, 2509–2513.

(12) (a) Hong, S.; Zhu, J.; Mirkin, C. A. *Science* **1999**, *286*, 523–528. (b) Piner, R. D.; Zhu, J.; Xu, F.; Hong, S.; Mirkin, C. A. *Science* **1999**, *283*, 661–663.

(13) (a) He, Q.; Kuller, A.; Grunze, M.; Li, J. *Langmuir* **2007**, *23*, 3981–3987. (b) Schmelmer, U.; Jordan, R.; Geyer, W.; Eck, W.; Golzhauser, A.; Grunze, M.; Ulman, A. *Angew. Chem., Int. Ed.* **2003**, *42*, 559–562.

(14) (a) Eck, W.; Stadler, V.; Geyer, W.; Zharnikov, M.; Golzhauser, A.; Grunze, M. *Adv. Mater.* **2000**, *12*, 805–808. (b) Golzhauser, A.; Eck, W.; Geyer, W.; Stadler, V.; Weimann, T. H.; Hinze, P.; Grunze, M. *Adv. Mater.* **2001**, *13*, 803–806.

(15) Westcott, N. P.; Pulsipher, A.; Lamb, B. M.; Yousaf, M. N. *Langmuir* **2008**, *24*, 9237–9240.

(16) Hoertz, P. G.; Niskala, J. R.; Dai, P.; Black, H. T.; You, W. *J. Am. Chem. Soc.* **2008**, *130*, 8763–9772.

(17) (a) Palyvoda, O.; Bordenyuk, A. N.; Yatawara, A. K.; McCullen, E.; Chen, C.-C.; Benderskii, A. V.; Auner, G. W. *Langmuir* **2008**, *24*, 4097–4106. (b) Chan, E. W. L.; Yousaf, M. N. *J. Am. Chem. Soc.* **2006**, *128*, 15542–15546. (c) Hoover, D. K.; Chan, E. W. L.; Yousaf, M. N. *ChemBioChem* **2007**, *8*, 1920–1923. (d) Yousaf, M. N.; Houseman, B. T.; Mrksich, M. *Proc. Natl. Acad. Sci. U.S.A.* **2001**, *98*, 5992–5996.

(18) Delamarche, E.; Michel, B.; Kang, H.; Gerber, C. *Langmuir* **1994**, *10*, 4103–4108.

(19) Kandere-Grzybowski, K.; Cambell, C.; Komarova, Y.; Grzybowski, B. A.; Borisy, G. G. *Nat. Methods* **2005**, *2*, 739–741.

(20) (a) Tosatti, S.; Textor, M. M.; Spencer, N. D. *Langmuir* **2002**, *18*, 3537–3548. (b) Hofer, R.; Textor, M.; Spencer, N. D. *Langmuir* **2001**, *17*, 4014–4020.

(21) (a) Zhu, F.; Zhang, K.; Guenther, E.; Jin, C. S. *Thin Solid Films* **2000**, *363*, 314–317. (b) Zhu, F.; Jennings, P.; Cornish, J.; Hefter, G.; Luczak, K. *Sol. Energy Mater. Sol. Cells* **1997**, *49*, 163–169.

(22) (a) Hodgson, L.; Chan, E. W. L.; Hahn, K. M.; Yousaf, M. N. *J. Am. Chem. Soc.* **2007**, *129*, 9264–9265. (b) Choi, C. K.; Margraves, C. H.; Jun, S. I.; English, A. E.; Rack, P. D.; Kihm, K. D. *Sensors* **2008**, *8*, 3257–3270. (c) Curreli, M.; Li, C.; Sun, Y.; Lei, B.; Gundersen, M. A.; Thompson, M. E.; Zhou, C. *J. Am. Chem. Soc.* **2005**, *127*, 6922–6923.

(23) (a) Van den Meerakker, J.; Jacobs, J. *J. Electrochem. Soc.* **1996**, *143*, L40–L42. (b) Pokela, R.; Toivanen, R.; Lindroos, V. *Key Eng. Mater.* **1987**, *20*−*28*, 3863–3873. (c) Lee, S.; Dongfang, Y.; Nikumb, S. *Appl. Surf. Sci.* **2007**, *253*, 4740–4747. (d) Ishikawa, F. N.; Chang, H.-K.; Koungmin, R.; Chen, P.-O.; Badmaev, A.; De Arco, L. G.; Shen, G.; Zhou, C. *ACS Nano* **2009**, *3*, 73–79.

(24) (a) Koide, Y.; Such, M. W.; Basu, R.; Evmenenko, G.; Cui, J.; Dutta, P.; Hersam, M. C.; Marks, T. J. *Langmuir* **2003**, *19*, 86–93. (b) Jeon, N. L.; Clem, P. G.; Nuzzo, R. G.; Payne, D. A. *J. Mater. Res.* **1995**, *10*, 2996–2999.

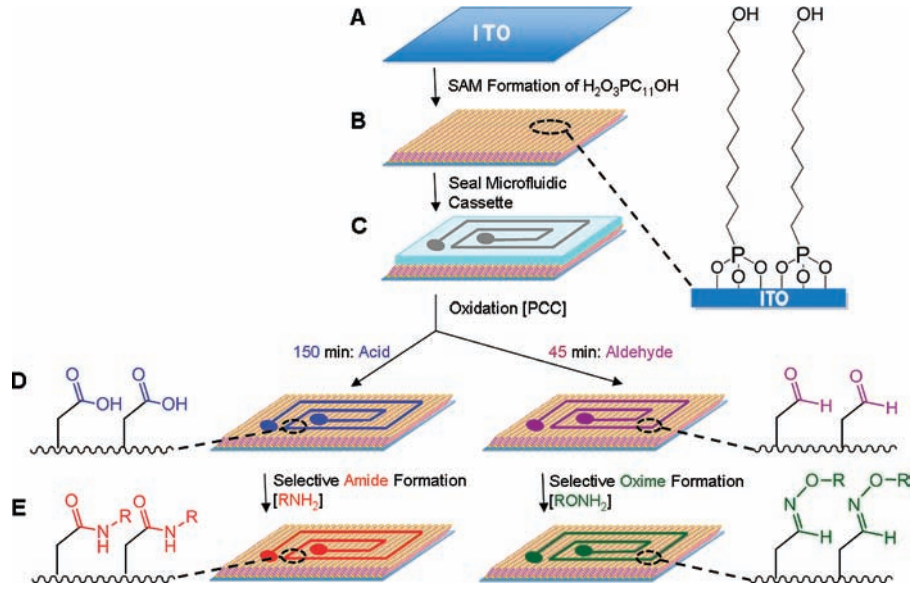

Figure 1. Schematic for the microfluidic oxidative activation of $H_2O_3PC_{11}OH$ SAMs on ITO with spatially controlled generation of aldehyde and carboxylic acid tail groups for subsequent chemoselective ligation. (A) An ITO substrate was sonicated in water, ethanol, and acetone. (B) In order to form a self-assembled monolayer, the substrate was submerged in a solution of $H_2O_3PC_{11}OH$ (1 mM) in water (16 h). (C) A microfluidic cassette was reversibly sealed to the surface, and PCC, a mild oxidant, in ACN was flowed through the microchannels to convert the alcohol-terminated SAM to aldehyde (45 min) or carboxylic acid tail groups (150 min). (D) After stamp removal, the patterned microchannels represented a 2D projection of aldehydes or acids on the surface. (E) For chemoselecitve immobilization of ligands to aldehyde- or acid-terminated surfaces, oxyamine ($RONH_2$)- or amine (RNH_2)-containing ligand were allowed to react on the surface and immobilized only to the oxidized regions. The resulting oxime and amide conjugates represented a high-fidelity 2D projection of the microchannels.

Scheme 1. Synthesis of 11-Hydroxyundecylphosphonic Acid[a]

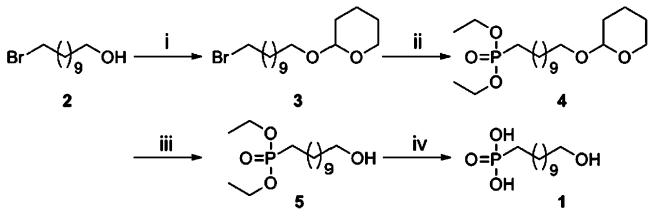

[a] Reagents and conditions: (i) dihydropuran, HCl, THF, rt, 12 h, 91%; (ii) triethylphosphite, 110 °C, 12 h, 74%; (iii) 3:1:1 AcOH:THF:H_2O, rt, 16 h, 61%; (iv) bromotrimethylsilane, DCM, rt, 6 h, 93%.

techniques to obtain 100 μm features) was reversibly sealed to the substrate.[25] Pyridinium chlorochromate (PCC, **10**, 300 mM in acetonitrile (ACN)) was then flowed through the microchannels and allowed to oxidize the hydroxy-terminated SAM. Dependent on the oxidative duration, surface hydroxyls could be converted to either aldehydes (45 min) or carboxylic acids (150 min). After aldehyde generation, oxyamine-containing ligands were chemoselectively immobilized to the surface, resulting in a covalent oxime bond. When exposed to PCC for 150 min, amide linkages were formed from reaction of acid tail groups with amine-containing ligands in the presence of *N*-hydroxysuccinimide (NHS) and dicyclohexyl carbodiimide (DCC). Thus, a single hydroxyl-terminated SAM on ITO could be chemically altered with the same oxidant and concentration to generate two different chemical functional groups that could be independently tailored by different chemoselective ligand immobilization strategies.

The uniformity of SAM formation, before as well as after chemical modification, was investigated by measuring the static

Table 1. Contact Angle Measurements of Hydroxy-, Aldehyde-, and Carboxylic Acid-Terminated Surface Groups on ITO

Surface Group			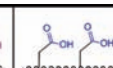
Contact Angle (°)	33.9 ± 0.40	52.9 ± 0.80	22.0 ± 2.0

contact angle of water on alcohol-, aldehyde-, and acid-terminated surfaces. Averages and standard deviations are reported in Table 1. Conditions favoring aldehyde generation correspond to larger contact angles than conditions forming carboxylic acids, as well as initial $H_2O_3PC_{11}OH$ SAMs, indicating that there was a uniform increase in hydrophobicity on the surface. On ITO, carboxylic acids can be formed by the longer oxidation duration required for transforming the hydroxyl-terminated SAM without monolayer desorption. A similar oxidation method was performed on gold surfaces containing SAMs of 11-mercapto-1-undecanol using PCC concentrations lower by 1000-fold, resulting solely in aldehydes. Higher concentrations or oxidizing durations longer than 70 min appeared to etch the gold and destroy the monolayer.[26] Therefore, carboxylic acid formation is compatible with alcohol-terminated SAMs on ITO but not SAMs of alkanethiols on gold, presumably due to the greater stability of the ITO−phosphonate linkage. Milder conditions and different oxidants are currently being investigated for the gold SAM surfaces.

To verify that both aldehydes and acids were being generated from the same alcohol-terminated SAM on ITO, cyclic voltammetry (CV) was performed. Figure 2 shows CV data from

(25) (a) Xia, Y.; Whitesides, G. M. *Annu. Rev. Mater. Sci.* **1998**, *28*, 153–184. (b) Weibel, D. G.; DiLuzo, W. R.; Whitesides, G. M. *Nat. Rev.* **2007**, *5*, 209–218. (c) Lahiri, J.; Ostuni, E.; Whitesides, G. M. *Langmuir* **1999**, *15*, 2055–2060.

(26) Lamb, B. M.; Westcott, N. P.; Yousaf, M. N. *ChemBioChem* **2008**, *9*, 2220–2224.

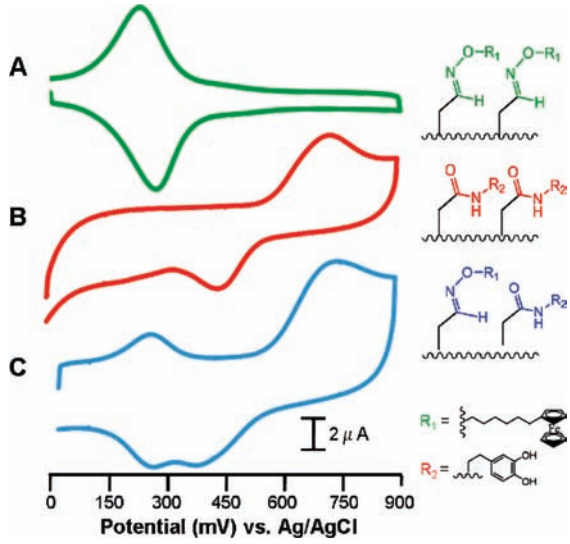

Figure 2. Electrochemical characterization of ferrocene-oxyamine and dopamine immobilized to surfaces presenting either aldehydes and acids or a combination of acids and aldehydes generated on SAMs of $H_2O_3PC_{11}OH$. (A) A cyclic voltammogram of ferrocene-oxyamine (green), with distinctive redox peaks of 230 and 270 mV, chemoselectively immobilized to aldehyde tail groups generated from oxidation of $H_2O_3PC_{11}OH$ on ITO. (B) A cyclic voltammogram of dopamine (red), with distinctive redox peaks of 360 and 730 mV, chemoselectively immobilized to carboxylic acid tail groups generated from oxidation of $H_2O_3PC_{11}OH$ on ITO. (C) A mixed surface containing both electroactive ligands immobilized to a surface presenting both aldehyde and carboxylic acid tail groups after oxidation of $H_2O_3PC_{11}OH$ on ITO.

surfaces that have been oxidized with conditions for aldehyde (300 mM PCC, 45 min) and acid (300 mM PCC, 150 min) generation, as well as a mixed aldehyde and acid surface (300 mM PCC, 70 min). Electroactive ferrocene-oxyamine (**6**, 30 mM in ethanol, 40 °C, 20 min) and dopamine (**8**, 300 mM in DMSO, 16 h) with NHS/DCC (150 mM) were immobilized to substrates following oxidation. Distinct redox peaks at 230 and 270 mV for ferrocene-oxyamine, and at 360 and 730 mV for dopamine, were observed from the resultant covalent oxime and amide linkages, respectively. As a control, dopamine was immobilized to surfaces oxidized for 45 min, and ferrocene-oxyamine was reacted on substrates that had been exposed to PCC for 180 min. Redox peaks were not present when scanned, indicating that no ligand immobilization occurred.

The percentage of aldehydes generated from hydroxy-terminated surfaces as a function of oxidation duration (0−45 min) was determined by integrating the redox peak areas corresponding to the CV data following ferrocene-oxyamine immobilization. These data were easily reproduced and used to calculate the kinetic rate profile of aldehyde production, fitted to pseudo-first-order kinetics. The aldehyde production rate was determined to be 0.11 min^{-1} as described previously.[13] Similarly, the acid production rate from aldehyde surfaces was found to be 0.018 min^{-1}. Substrates were oxidized for longer durations beyond approximate complete aldehyde conversion (45−150 min), and the CV data were generated after redox-active ferrocene-oxyamine and dopamine immobilization was analyzed. The rate of the disappearance of aldehydes corresponds approximately with the rate of production of acids, calculated to be 0.018 min^{-1} with error as reported (Figure 3). Therefore, oxidation over the substrate can be controlled to generate aldehydes and acids, as well as a mixture of the two groups.

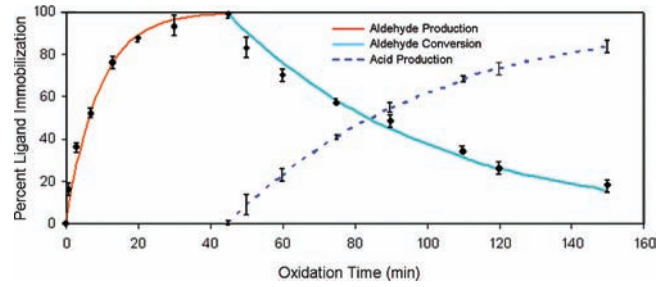

Figure 3. Kinetic characterization of aldehyde and acid production on ITO using redox-active immobilization ligands ferrocene-oxyamine (for aldehyde) to generate oximes and dopamine (for carboxylic acids) to generate amides. Percent ligand immobilization versus oxidation time (300 mM PCC, ACN, 0−150 min) plot for SAMs of $H_2O_3PC_{11}OH$ with calculated pseudo-first-order rates of 0.11 min^{-1} for aldehyde production (red) and 0.018 min^{-1} for aldehyde disappearance or conversion to acid (blue) and acid production (dotted blue). The acid production rate is approximately the same as the rate of disappearance of aldehydes.

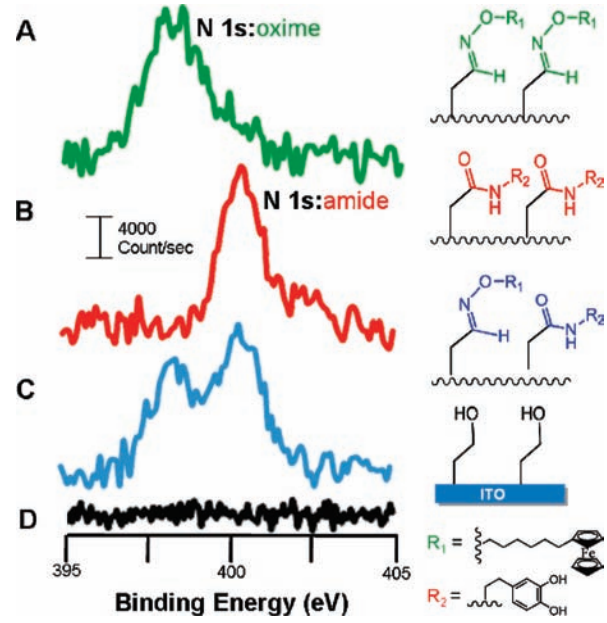

Figure 4. X-ray photoelectron spectroscopy characterization of oxime and amide bonds on ITO. Surfaces presenting SAMs of $H_2O_3PC_{11}OH$ were oxidized to generate aldehyde or carboxylic acid tail groups for subsequent chemoselective ligation and XPS analysis. (A) The nitrogen 1s peak observed at 398 eV corresponds to the oxime nitrogen of ferrocene-oxyamine-immobilized aldehyde-presenting surfaces. (B) The nitrogen 1s peak observed at 400 eV corresponds to the amide nitrogen of dopamine immobilized to carboxylic acid-presenting surfaces. (C) A mixed surface of ferrocene-oxyamine and dopamine ligands, showing both nitrogen peaks of oxime and amide bonds, respectively. (D) An unoxidized ITO surface presenting a SAM of $H_2O_3PC_{11}OH$, showing no nitrogen present.

X-ray photoelectron spectroscopy (XPS) was also performed to examine the amide and oxime nitrogen bound to the SAM on the surface. Hydroxy-terminated SAMs on ITO were oxidized for 45, 70, and 150 min, followed by subsequent selective immobilization of ferrocene-oxyamine and dopamine. (Figure 4) The nitrogen 1s peak representing the oxime linkage between ferrocene-oxyamine and aldehydes was observed at 398 eV, corresponding to data seen with gold SAMs.[17] Similarly, the nitrogen 1s peak of the amide resultant from conjugation of dopamine to acid was observed at 400 eV. This peak correlated well with the XPS data produced by dopamine immobilization to SAMs of carboxylic acid-terminated phosphonate (Fluka) on ITO. Also, substrates were oxidized for 70

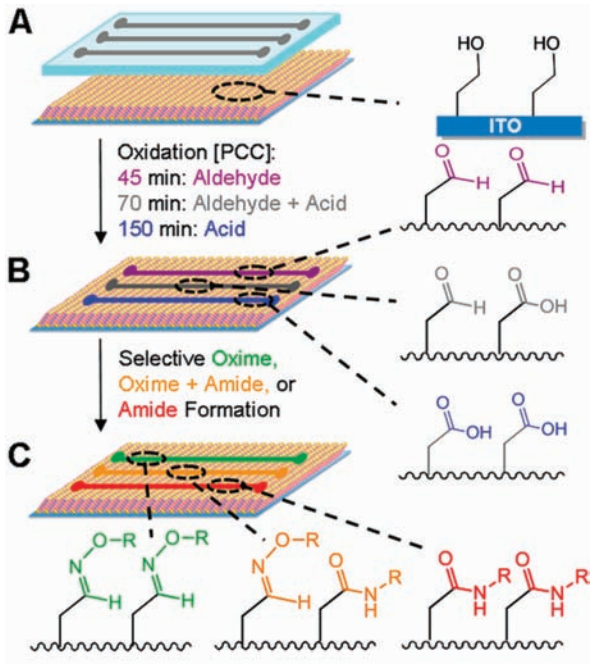

Figure 5. Schematic for the oxidative activation of $H_2O_3PC_{11}OH$ SAMs on ITO for controlled generation of aldehyde, carboxylic acid, and a mixed surface of both aldehyde and acid tail groups for subsequent chemoselective ligation. (A) A microfluidic cassette with separate channels was reversibly sealed to an ITO surface containing SAMS of $H_2O_3PC_{11}OH$. (B) PCC in ACN was flowed through the microchannels in order to convert the alcohol-terminated SAM to aldehyde (45 min), mixed aldehyde and acid (70 min), or acid tail groups (150 min). (C) To functionalize the surface, oxyamine-, amine-, and a mixture of oxyamine- and amine-containing ligands were chemoselectively immobilized to regions presenting aldehyde, acid, or a mixture of aldehydes and acids on the surface.

min, generating mixed aldehyde and acid surfaces, followed by immobilization of ferrocene-oxyamine and dopamine ligands. Again, the nitrogen 1s peaks appeared at 398 and 400 eV, respectively, verifying that both ligands were immobilized on the same substrate. Controls including unoxidized SAMs of $H_2O_3PC_{11}OH$ on ITO, dopamine immobilized onto surfaces that had been oxidized for 45 min, and ferrocene-oxyamine immobilized onto substrates with exposure to PCC for 180 min showed no nitrogen present.

Atomic force microscopy (AFM) was also used to characterize SAM formation and chemical modification. Lateral force microscopy (LFM) images of bare ITO, a hydroxy-terminated SAM, a mixed aldehyde- and acid-terminated SAM after oxidation with PCC, and immobilized ferrocene-oxyamine and dopamine on ITO are shown (Supporting Information). Without SAM formation, ITO is characteristically rough. LFM images display that there is less contrast in surface friction due to more uniformity in the chemical environment after SAM modification.

To exhibit the diversity in performing this dual-orthogonal strategy to spatially control the immobilization of the oxyamine- and amine-containing ligands on ITO, fluorescent compounds were patterned by microfluidics and then visualized by fluorescence microscopy (Figure 5). A microfluidic cassette with separate channels was reversibly sealed to an ITO surface containing SAMs of $H_2O_3PC_{11}OH$, and oxidation with PCC was carried out as previously described. Following oxidation, a mixture of Alexa 488-oxyamine (**7**) and Rhodamine (**9**) was allowed to react on the surface. When imaged, the immobilized fluorescent dyes produced a 2D projection of the microchannels,

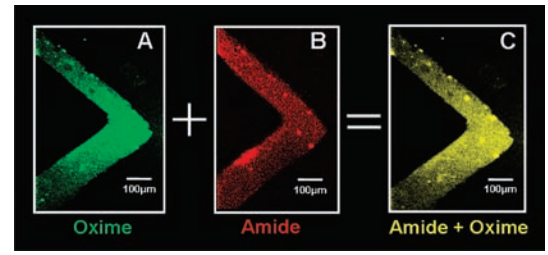

Figure 6. Fluorescent micrographs of a mixed aldehyde and carboxylic acid-presenting surface patterned by microfluidic oxidation (PCC, 70 min) followed by chemoselective oxime and amide immobilization. Ligands were imaged directly on the surface. (A) Alexa 488-oxyamine immobilized to aldehyde surface groups generated by microfluidic oxidation with PCC in ACN. (B) Rhodamine immobilized to carboxylic acid surface groups generated by microfluidic oxidation on the same pattern. (C) A combined image of the pattern showing a mixed surface containing both oxime and amide conjugates generated by rapid and straightforward microfluidic oxidaton of a hydroxy-presenting ITO surface.

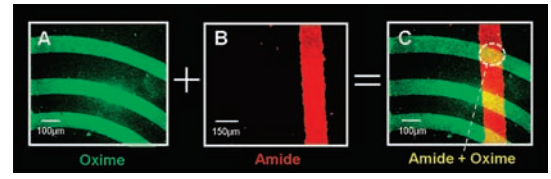

Figure 7. Fluorescent micrographs of patterned zones of aldehyde and carboxylic acid generated by serial microfluidic oxidation followed by chemoselective oxime and amide immobilization to ITO surfaces. (A) Immobilized Alexa 488-oxyamine after selective microfluidic oxidation conditions to generate aldehyde surface groups in a spiral pattern. (B) Immobilized Rhodamine in a bar pattern after selective microfluidic oxidation to generate acid surface groups in the same region. (C) A combined image of the region displaying a dual-patterned surface containing both oxime and amide conjugates, as well as the overlap upon mixing.

and patterns of oxime (green), amide (red), and a mixture of oxime and amide (yellow) conjugates were observed (Figure 5). More specifically, both carboxylic acids and aldehydes were generated with spatial control on an ITO substrate. PCC was allowed to react in the microchannels for 70 min, resulting in mixture of acids and aldehydes projected from the surface. Rhodamine (7 mM in DMSO, 3 h, 75 °C) followed by Alexa 488-oxyamine (4 mM in DMSO, 1 h) were immobilized. In addition, a single substrate is displayed in Figure 6 with a pattern of two dyes: Alexa 488-oxyamine (A, green), rhodamine (B, red), with a superimposed image showing the same mixed region (C, yellow).

Alternatively, spatially controlled generation of aldehydes and carboxylic acids independently is also possible by using different microfluidic cassettes for patterning ligands on the same surface (Figure 7). Beginning with one cassette on a SAM of $H_2P_3OC_{11}OH$, substrates were oxidized for 45 min in order to generate aldehydes, followed by immobilization of Alexa 488-oxyamine within the microchannels (4 mM in DMSO, 1 h, 75 °C). The Alexa 488-oxyamine immobilized to aldehydes present, resulting in a clear projection of the pattern. After rinsing and removing the cassette, a different cassette was reversibly sealed to the surface, and PCC was left to react for 150 min in order to generate acids for subsequent rhodamine immobilization within the channels (7 mM in DMSO, 3 h, 75 °C). Rhodamine immobilized to the newly formed acids. When visualized using fluorescence microscopy, two distinct oxime (green, Figure 7A) and amide (red, Figure 7B) patterns were observed, with overlapping

regions containing a mixture of both oxime- and amide-conjugated ligands (yellow, Figure 7C).

Conclusion

In this report we show the development of a new strategy to pattern ligands onto a surface. We activate a simple hydroxy-terminated SAM surface with a rapid, inexpensive, and mild microfluidic oxidation strategy to generate chemoselective and patterned ITO surfaces. This method allows the use of two orthogonal strategies for selective ligand immobilization with spatial control originating from a single SAM composition on ITO. Aldehyde and carboxylic acid surface groups were generated by oxidation of alcohol-terminated SAMs followed by immobilization and characterization of a variety of oxyamine- and amine-containing compounds. Microfluidic patterning provides spatial control of aldehydes and acids on the surface, as well as resulting oxime and amide conjugates, respectively. Taking advantage of the robust, conductive, and transparent nature of ITO, oxime and amide linkages were characterized by CV, XPS, AFM, and fluorescence microscopy. The ability to spatially control and pattern the generation of mixed aldehyde and carboxylic acid surfaces as well as distinct regions of carboxylic acids and aldehydes for subsequent immobilization of ligands would greatly benefit research fields such as cell biology and molecular electronics. This new surface patterning strategy circumvents multistep syntheses and is applicable to tailoring a variety of other materials. Ongoing research includes exploring multiple ligand immobilization for co-culture studies and cell migration studies and for generating high-throughput ligand microarrays on nickel and other metal oxide surfaces.

Experimental Section

Fluorescent dyes were obtained from Invitrogen; all other chemicals were obtained from Sigma Aldrich. Indium tin oxide slides were purchased from Nanocs (New York, NY).

Synthesis. Ferrocene-oxyamine (**2**) was synthesized as previously reported.[15]

2-(11-Bromoundecyloxy)tetrahydro-2*H*-pyran (3). To a solution of **2** (4.00 g, 15.9 mmol) in THF (40 mL) were added dihydropuran (6.54 mL, 71.1 mmol) and HCl (3 drops). The reaction was stirred under inert atmosphere (N_2) for 12 h and was then washed with sodium bicarbonate (3 × 25 mL) and brine (1 × 25 mL). The mixture was purified by flash chromatography (9:1 Hex:EtOAc) and concentrated to afford a colorless oil **3** (4.84 g, 91%). ^{1}H NMR (400 Hz, $CDCl_3$, δ): 4.58 (t, 1H, $J = 8$; CH), 3.86−3.75 (m, 2H, $J = 7$; CH_2), 3.52 (m, 1H, $J = 8$; CH), 3.41−3.38 (m, 3H, $J = 7$; CH, CH_2), 1.87−1.84 (m, 3H, $J = 7$; CH, CH_2), 1.58 (m, 1H, $J = 8$; CH), 1.55 (m, 6H, $J = 7$; CH_2), 1.43−1.40 (m, 2H, $J = 7$; CH_2), 1.29 (m, 12H, $J = 7$; CH_2).

Diethyl 11-(Tetrahydro-2*H*-pyran-2-yloxy)undecylphosphonate (4). A solution of **3** (3.24 g, 9.66 mmol) in neat triethylphosphite (9.85 mL, 53.1 mmol) was refluxed at 110 °C under inert atmosphere (N_2) for 12 h. The mixture was concentrated and purified by flash chromatography (1:1 Hex:EtOAc, eluted **3** with 100% MeOH) to afford a colorless oil **4** (2.98 g, 74%). ^{1}H NMR (400 Hz, $CDCl_3$, δ): 4.57 (t, 1H, $J = 7$; CH), 3.83−3.81, (q, 4H, $J = 9$; CH_2), 3.72−3.68 (m, 2H; CH_2), 3.48−3.39 (m, 2H, $J = 7$; CH_2), 1.81 (m, 1H, $J = 9$; CH), 1.68−1.59 (m, 3H, $J = 8$; CH, CH_2), 1.53−1.52 (m, 7H, $J = 11$, $J = 7$; CH, CH_2), 1.32−1.30 (m, 18H, $J = 7$; CH_2, CH_3).

Diethyl 11-Hydroxyundecylphosphonate (5). To solution of acetic acid, water, and THF (3:1:1 30 mL, 10 mL, 10 mL) was added **4** (0.800 g, 2.00 mmol). The mixture was stirred under inert atmosphere (N_2) for 16 h. After completion, the mixture was concentrated, diluted with EtOAc, and washed with 0.01 M NaOH (3 × 25 mL) to afford a colorless oil **5** (0.379 g, 61%). ^{1}H NMR (400 Hz, $CDCl_3$, δ): 4.09−4.05 (q, 4H, $J = 9$; CH_2), 3.62−3.59 (t, 2H, $J = 7$; CH_2), 2.55 (s, 1H; O−H), 1.70−1.66 (m, 2H, $J = 8$; CH_2), 1.56−1.53 (m, 4H, $J = 7$; CH_2), 1.32−1.26 (m, 18H, $J = 7$, $J = 7$; CH_2, CH_3).

11-Hydroxyundecylphosphonic Acid ($H_2O_3PC_{11}OH$, 1). To a solution of **5** (0.379 g, 0.12 mmol) in dry CH_2Cl_2 (15 mL) was added trimethylbromosilane (0.50 mL, 3.6 mmol). The mixture was stirred under inert atmosphere (N_2) for 6 h. After completion, the mixture was concentrated and stirred with MeOH (20 mL) under N_2 for 2 h. The mixture was then concentrated to a colorless oil and recrystallized with acetone to afford a white solid **1** (0.288 g, 93%).^{1}H NMR (400 Hz, MeOD, δ): 3.51 (t, 2H, $J = 7$; CH_2), 1.82−1.80 (m, 2H, $J = 7$; CH_2), 1.58−1.48 (m, 6H, $J = 8$; CH_2), 1.30 (m, 12H, $J = 7$; CH_2). HRMS (ESI, *m/z*): [M − H] calcd for $C_{11}H_{25}O_4P$, 252.2876; found, 251.1.

Microfabrication. Microfluidic cassettes were fabricated using soft lithography.[25] Patterns were achieved using masks drawn in Adobe Illustrator CS3 and photoplotted by Page works onto Mylar sheets. SU-8 50 (Microchip) was patterned using the manufacturer's directions to obtain 100 μm channel depth. The Sluggard 184 (Dow Corning) was prepared in a 3:20 curing agent:elastomer (PDMS). The prepolymer was cast over the mold, degassed for 30 min, and cured for 1 h at 75 °C. The PDMS was then removed from the master, and access holes were added to the PDMS to allow fluid flow.

Preparation of ITO and SAM Formation. Indium tin oxide-coated (10 nm) slides (1 in. × 3 in. × 1.1 mm, 10 Ω/sq) were obtained from Nanocs. The slides were cut into 1 × 2 cm^2 pieces and sonicated in diionized water, ethanol, and acetone each for 20 min. Surfaces were then rinsed with ethanol and dried. In order to form SAMs on ITO, the slides were immersed in a 1 mM solution of 11-hydroxyundecylphosphonic acid in water for at least 16 h. Once removed from solution, the surfaces were rinsed with ethanol and dried before use.

Electrochemical Characterization. All electrochemical experiments were performed using a Bioanalytical Systems CV-100W potentiostat. Electrochemical data were obtained in a 1 M $HClO_4$ electrolyte solution with an Ag/AgCl electrode (Bioanalytical Systems) serving as the reference, the ITO monolayer as the working electrode, and a Pt wire as the counter electrode. Surfaces were scanned at a rate of 100 mV/s. All electrochemical measurements were performed in trials of four, with the average and standard deviation reported.

Ferrocene-Oxyamine and Dopamine Immobilization. Surfaces containing SAMs of 11-hydroxyundecylphosphonic acid were oxidized using a 300 mM solution of PCC in ACN for either 45 min to generate aldehyde tail groups or 150 min to generate carboxylic acid tail groups. Surfaces were then rinsed with ethanol and dried. A 30 mM solution of ferrocene-oxyamine in ethanol was allowed to react on the aldehyde surface for 20 min at 40 °C. To immobilize dopamine, a solution of 150 mM NHS, 150 mM DCC, and 300 mM dopamine in DMSO was allowed to react on the surface for 16 h at room temperature. Once the immobilization was complete, the surfaces were rinsed with ethanol and dried before verification by CV.

Kinetic Characterization of Aldehyde and Acid Production. The amount of ferrocene-oxyamine immobilized, corresponding to the total charge (Q) on the surface, was quantified by integrating the redox peak area observed from the CV data. The total charge was then compared to the theoretical value generated from a 100% converted surface using $Q = nFA\Gamma$ (where Q is the total charge, n is the number of electrons involved in the reaction (in this case, 1), F is Faraday's constant, and Γ is the surface coverage in molecules per surface area). The theoretical value was calculated to be 16.1 $\mu C/cm^2$ for a surface density of 1.66×10^{-10} mol/cm.[2] The density of both aldehydes and ligand on the surface could be controlled by varying the PCC reaction

Scheme 2. Structures of Surface Groups and Oxyamine- and Amine-Containing Ligands for Chemoselective Immobilization to ITO Activated Surfaces

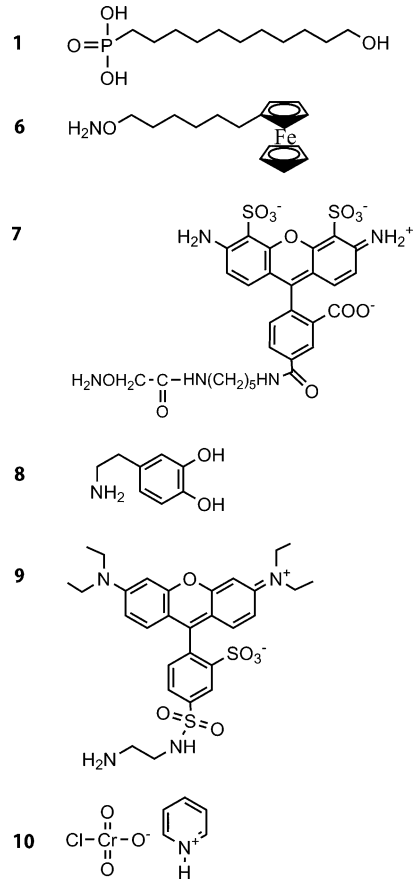

duration. It was found that by 45 min there was an approximately complete conversion to aldehyde groups. Similarly, oxidation times were extended from 45 to 150 min, and the amount of ferrrocene-oxyamine and dopamine immobilized was calculated by CV analysis. Each data point (0−150 min) was performed at least four times, and the amount of ferrocene-oxyamine immobilized was calculated as reported above. Averages and percent error were also determined. Based on the CV data, the theoretical and actual amounts of ligand bound were compared and used to construct a relationship between the percent of ligand immobilized and oxidation time, as shown in Figure 3. The error bars shown represent the standard deviation within each time point measured. Rate profiles were fitted to pseudo-first-order kinetics, and rates were determined to be 0.11 min^{-1} for aldehyde production and 0.018 min^{-1} for acid production.

Patterned Mixed Aldehyde and Carboxylic Acid Surface by Microfluidic Oxidation of Alcohol-Terminated SAMs. A PDMS microfluidic cassette was reversibly placed on an ITO surface containing a SAM of 11-hydroxyundecylphosphonic acid (**1**). A 300 mM solution of PCC in ACN was flowed through the channels and allowed to react for 70 min. Without removing the cassette, the reaction was quenched, and the surface and cassette were rinsed by flowing ethanol through the channels. A solution of 4 mM Alexa 488-oxyamine (Invitrogen), 150 mM NHS, 150 mM DCC, and 7 mM Rhodamine (Invitrogen) in DMSO was allowed to react with the surface for 3 h at 75 °C. The reaction was then quenched by submerging the surface in DMSO and was rinsed with ethanol and dried.

Dual-Patterned Surface by Microfluidic Oxidation of Alcohol-Terminated SAMs. A PDMS microfluidic cassette was reversibly placed on an ITO surface containing a SAM of 11-hydroxyundecylphosphonic acid. A 300 mM solution of PCC in ACN was flowed through the channels and allowed to react for 45 min to exclusively generate aldehydes. Without removing the cassette, the reaction was quenched, and the surface and cassette were cleaned by flowing ethanol through the channels. With the cassette still in place, a solution of 4 mM Alexa 488-oxyamine in DMSO was flowed through the channels and allowed to react for 1 h at 75 °C to generate the oxime conjugate. The reaction was quenched, and the PDMS microfluidic cassette was removed. A different PDMS microfluidic cassette pattern was then reversibly sealed to the same ITO surface containing patterned Alexa 488-oxyamine and unactivated regions of 11-hydroxyundecylphosphonic acid. The immobilization procedure was repeated as described previously, with the exception of PCC oxidation for 150 min to generate only carboxylic acids followed by reaction with a solution of 150 mM NHS, 150 mM DCC, and 7 mM Rhodamine in DMSO for 3 h at 75 °C to form the interfacial amide conjugate.

Fluorescence Microscopy. After patterning and immobilization of fluorescent ligands, ITO surfaces were imaged directly by fluorescent and brightfield microscopy using a Nikon TE2000E inverted microscope. Image acquisition and processing was carried out with Metamorph software. To show the overlay of both fluorescent dyes, images were taken of the same patterned region in separate light filters and combined into one image.

X-ray Photoelectron Spectroscopy. Ferrocene-oxyamine-, dopamine-, and mixed-functionalized surfaces were prepared as previously described. XPS measurements were performed on surfaces containing the immobilized ligands mentioned, as well as bare ITO and SAMs of 11-hydroxyundecylphosphonic acid with a Kratos Axis Ultra DLD. A mono Al anode source was used with a specific excitation energy of 1486.6 eV, and an 80 eV pass energy was used for the high-resolution scans. All binding energies are referenced to the C 1s of a saturated hydrocarbon at 284.7 eV.

Contact Angle Measurement. ITO surfaces containing SAMs of 11-hydroxyundecylphosphonic acid were oxidized with 300 mM PCC in ACN ranging from 0 to 150 min. The static contact angles of these reacted surfaces were measured using 10 μL drops of deionized H_2O using a KSV CAM 200 instrument and software. Measurements were performed in sets of eight for alcohol-, aldehyde-, and acid-terminated surfaces. Contact angle data were averaged, with the standard deviation shown in Table 1.

Atomic Force Microscopy. AFM images were obtained by using a MFP-3D Stand Alone atomic force microscope (Asylum Research, Santa Barbara, CA). Lateral force images were acquired in contact mode, using a silicon tip (0.03−0.08 N/m, MikroMasch USA, Wilsonville, OR), at a scan rate of 1 Hz, under ambient conditions. Four scans were performed on each substrate during the different stages of SAM manipulation to conclude the surface friction uniformity.

Acknowledgment. We thank Diana Hoover for her help in obtaining the AFM data. This work was supported by the Carolina Center for Cancer Nanotechnology Excellence and grants from the NCI to M.N.Y. and the Burroughs Wellcome Foundation (Interface Career Award).

Supporting Information Available: Lateral force microscopy images of different SAM compositions and bare ITO. This material is available free of charge via the Internet at http://pubs.acs.org.

JA809380E